



Fluorimetric detection of Sn^{2+} ion in aqueous medium using Salicylaldehyde based nanoparticles and application to natural samples analysis



Kishor S. Patil ^a, Prasad G. Mahajan ^b, Shivajirao R. Patil ^{b,*}

^a Dr. Babasaheb Ambedkar Technological University, Lonere, Dist: Raigad, Maharashtra, India

^b Fluorescence Spectroscopy Research Laboratory, Department of Chemistry, Shivaji University, Kolhapur- 416004, Maharashtra, India

ARTICLE INFO

Article history:

Received 18 December 2015

Received in revised form 4 July 2016

Accepted 10 July 2016

Available online 12 July 2016

Keywords:

Schiff base

2-[(E)-(2-phenylhydrazinylidene)methyl]phenol nanoparticles (PHPNPs)

Fluorescence enhancement

Excited state complex

Sn^{2+} detection

ABSTRACT

The fluorescent 2-[(E)-(2-phenylhydrazinylidene)methyl]phenol nanoparticles (PHPNPs) were prepared by a simple reprecipitation method. The prepared PHPNPs examined by Dynamic Light Scattering show narrower particle size distribution having an average particle size of 93.3 nm. The Scanning Electron Microphotograph shows distinct spherical shaped morphology of nanoparticles. The blue shift in UV-absorption and fluorescence spectra of PHPNPs with respect to corresponding spectra of PHP in acetone solution indicates H- aggregates and Aggregation Induced Enhanced Emission (AIEE) for nanoparticles. The nanoparticles show selective tendency towards the recognition of Sn^{2+} ions by enhancing the fluorescence intensity preference to Cu^{2+} , Fe^{3+} , Fe^{2+} , Ni^{2+} , NH_4^+ , Ca^{2+} , Pb^{2+} , Hg^{2+} and Zn^{2+} ions, which actually seem to quench the fluorescence of nanoparticles. The studies on Langmuir adsorption plot, fluorescence lifetime of PHPNPs, DLS-Zeta sizer, UV-visible and fluorescence titration with and without Sn^{2+} helped to propose a suitable mechanism of fluorescence enhancement of nanoparticles by Sn^{2+} and their binding ability during complexation. The fluorescence enhancement effect of PHPNPs induced by Sn^{2+} is further used to develop an analytical method for detection of Sn^{2+} from aqueous medium in environmental samples.

© 2016 Elsevier B.V. All rights reserved.

1. Introduction

A variety of new functionalized compounds which exhibit excellent fluorescent properties are of current interest in the development of systems for detection of metal ions in aqueous media [1–3]. The design and synthesis of such compounds capable of binding and sensing metal ions selectively received more attention in recent years due to important roles of these ions in many chemical and biological processes. Although many simple fluorophores have been used for development of sensory system in the past but possibilities like narrow excitation and broad emission spectra are the hurdles in use of these fluorophores towards particular metal ion detection. However compared to these traditional fluorophores, nanoparticles based sensors are more advantageous due to their characteristics like resistance to photo bleach, broad absorption spectrum and narrow enhanced emission spectrum. Because of the size dependent, tunable photoluminescence properties of organic nanoparticles, they are evolving as promising materials for sensor development [4–7]. The sensor material should be soluble in pure water to develop an efficient method for biological and environmental sample analysis. The aqueous insolubility of the hydrophobic fluorescent chemo sensors limits the application and hence new approach encompasses to prepare

aqueous suspension of nanoparticles. Fluorescent organic nanoparticles of functionalized molecules specifically binding with certain analyte are of great importance with improved sensitivity, selectivity and low detection limit because of strong aggregation induced enhanced emission (AIEE) [8–11]. The advantage of using fluorescent organic nanoparticles is the high surface area of nanoparticles and electrostatic attraction responsible for adsorption of analyte molecule on the specifically modified surface [10,11].

In recent years, a considerable scientific approach has been drawn to devise fluorescent organic nanoparticles (FONs) based sensors which selectively recognize various metal ions [12]. Although several analytical methods such as atomic absorption spectroscopy (AAS), inductively coupled atomic emission spectroscopy and inductively coupled plasma mass spectroscopy (ICP-AES and ICP-MS) have been widely used to detect metal ions [13]. The fluorescence spectroscopy is infinitely preferable due to easy handling, less expensive, appreciating sensitivity and fast response. Despite many impressive advances in AIEE based FONs, more facile preparation method without complex synthesis and expensive reactant is still highly demanded. The reprecipitation method is one of the suitable and economic method so far widely used to prepare FONs [14]. Many of the metal ions play very important roles in living system. The excess consumption of metal ion in body may cause serious infection in human metabolism [15]. Therefore it is today's need to develop a sensitive and selective method for the detection of metal ion in

* Corresponding author.

E-mail address: srp_fsl@rediffmail.com (S.R. Patil).

aqueous medium. Fluorescence probes based on Schiff base units have been developed and applied in the field of metal ion recognition in recent years. The development and application of Schiff base compounds with –N and –O as hard-base donor sites provide a facile pathway for binding towards metal ion in aqueous media [16–18]. We believe that the development of Schiff base centered nanoparticles based sensory system with controlled and regulation in properties can be used to detect metal ions and explored in field applications. Schiff base derivatives are known to coordinate with metal ions and exhibit enhanced optical properties of probe. In contrast to fluorescence quenching, the optical probes based on fluorescence enhancement effect are more advantages due to strong output signal arising from the system [19,20]. Therefore, it is proposed to synthesize Schiff base 2-[(E)-(2-phenylhydrazinylidene)methyl]phenol (PHP) to explore its use in the form of nanoparticles in sensing of metal ion. The metal ion recognition test performed using aqueous suspension of nanoparticles of PHP showed that presence of tin (Sn^{2+}) ion solution enhances the fluorescence of PHP nanoparticles while other ions namely Cu^{2+} , Fe^{3+} , Fe^{2+} , Ni^{2+} , NH_4^+ , Ca^{2+} , Pb^{2+} , Hg^{2+} and Zn^{2+} actually quench the fluorescence. The selective sensing and detection of tin ion from aqueous solution by fluorescence change of organic nanoparticles are discussed in this present paper.

Tin is a soft, white, silvery metal that is insoluble in water. Tin is a metal that can combine with other chemicals to form various compounds which are water soluble. Tin poisoning refers to the toxic effects of tin and its compounds. Tin can enter human body when food or drinks with contaminated water is consumed which has tin in it [21]. The University of Medical Sciences in Iran investigated in vitro effects of several metals, including tin, on sperm creatine kinase. Reduced sperm metabolism was observed which is believed to be a cause of infertility in men. The water soluble tin complex can irritate the skin and delicate tissue, particularly the eyes and respiratory system. The contaminated water with tin content was found to be extremely toxic to human embryonic kidney cells, energy metabolism and brain function by interfering with neurotransmitters. Therefore it is a current need to develop a highly selective and sensitive method for the determination of Sn^{2+} in aqueous medium. In this paper, we report a synthesis and characterization of Schiff-base compound for preparation of its nanoparticles by reprecipitation method. Further, nanoparticles that are explored as novel nano probe for the detection of Sn^{2+} in aqueous media depend on fluorescence enhancement studies. The present method was successfully applied to quantitative determination of Sn^{2+} in collected environmental samples.

2. Experimental

2.1. Materials

Salicylaldehyde and Phenyl hydrazine were obtained from Sigma Aldrich (India). The required metal salts viz. SnCl_2 , CuCl_2 , FeCl_3 , FeCl_2 , NiCl_2 , NH_4Cl , CaCl_2 , PbCl_2 , HgCl_2 and ZnCl_2 used as sources were procured from Spectrochem Pvt. Ltd. Mumbai, (India) and were used as received. Analytical grade acetone and ethanol (S. D. Fine Chemicals, Mumbai, India) were used after distillation. Ultrapure water was obtained by passing distilled water through a Millipore unit (India) and used in preparation of solution required for fluorescence experiments.

2.2. Instruments for Characterization

^1H (300 MHz) and ^{13}C (75 MHz) NMR spectra were recorded in CDCl_3 on Bruker Avance 300 NMR spectrophotometer. Chemical shifts were reported using tetramethylsilane (TMS) as an internal standard. Infrared spectrum was recorded in KBr pallets on a Perkin Elmer FT-IR spectrophotometer in the 4000–400 cm^{-1} region. Mass spectrum was recorded using Agilent 1200 series LC and 6130 series Single Quadrupole MS systems instrument. UV–visible spectra and Fluorescence spectra of the solutions were recorded on a Shimadzu

spectrophotometer and on a JASCO FP-750 spectrofluorometer, respectively. The size and zeta potential of the PHPNPs were measured using a Malvern Zetasizer (nano ZS-90) equipped with a 4 mW, 633 nm He–Ne Laser (U.K.) at 25 °C under the fixed angle of 90° in disposable polystyrene cuvettes. The morphology of PHPNPs was assessed by Scanning Electron Microscope (SEM), (JEON-6360 Japan), operated at an accelerating voltage of 20 kV. The pH of the aqueous suspension of nanoparticles was measured on LI120 digital pH meter instrument. The fluorescence lifetimes measured by time correlated single photon counting method for which a time resolved fluorescence spectrometer (Horiba Jobin Yvon IBH) was used equipped with nanosecond LEDs (420 nm).

2.3. Synthesis of 2-[(E)-(2-phenylhydrazinylidene)methyl]phenol: (PHP)

PHP was synthesized using reported procedure [22,23]. The synthesis route performed is shown in Scheme 1. Salicylaldehyde (0.1 mmol) was dissolved in 20 mL ethanol and a solution 0.1 mmol phenyl hydrazine was added. The resulting mixture was stirred on a magnetic stirrer for 30 min. The pale yellow solid thus obtained was filtered, washed with distilled water and dried. The final product was recrystallized from hot ethanol solution and was characterized to be used further for preparation of nanoparticles in aqueous suspension.

2.4. Spectral Characterization of PHP

The formation of product was confirmed by spectral techniques viz. IR, ^1H , ^{13}C NMR and MS analysis. Pale yellow powder; IR (Fig. S1, ES $^+$): 3290 cm^{-1} , Presence of –NH, 1602 indicates the presence of $\text{C}=\text{N}$; ^1H NMR (300 MHz, CDCl_3 , Fig. S2, ES $^+$): δ 10.88 (1H, s, –NH), δ 7.90 (1H, s, –OH), δ 7.53–7.59 (1H, d, J = 18 Hz, –CH), δ 6.90–7.35 (9H, m, Ar–H); ^{13}C NMR (75 MHz, CDCl_3 , Fig. S3, ES $^+$): $\text{C}=\text{O}$, δ 157.06 (C - 1); δ 143.40 (C - 11), δ 143.20 (C - 8) 112.65–130.4 (Ar - C); MS (EI) (Fig. S4, ES $^+$): 213.9 [M] $^+$ m/z. The IR spectrum exhibited bands at 3290 cm^{-1} for NH stretching, while band detected at 1602 cm^{-1} are due to stretching of $\text{>C}=\text{N}$. In ^1H NMR spectrum, a significant singlet at δ 10.88 ppm confirmed the presence of –NH protons. Singlet depicted at δ 7.90 ppm highlighted presence of –OH, and doublet at δ 7.56 ppm is due to –CH protons. In ^{13}C NMR –C=N carbon appeared at δ 143.20 ppm while the carbon adjacent to OH appeared at 157.06 ppm. Mass spectrum that displayed a strong peak at 213.9 m/z for [M] $^+$ is also in good agreement with the molecular ion peak of proposed structure.

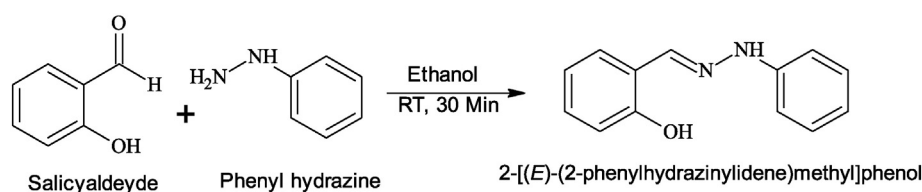
2.5. Preparation of PHPNPs

Nanoparticles of PHP were prepared using simple and efficient reprecipitation method [15] developed in the laboratory. 5 mL solution of PHP in acetone (5 mM) was injected into 250 mL water (Millipore) by using micro syringe. The whole solution was vigorously stirred by magnetic stirrer for 1 h and sonicated for 30 min to disperse the nanoparticles in aqueous medium. Pale yellow colored transparent suspension of nanoparticles was then undertaken for particle size distribution analysis and surface morphology examination.

3. Results and Discussion

3.1. Particle Size and Morphology of PHPNPs

Fig. 1 shows particle size distribution histogram of PHPNPs taken on the Malvern Zetasizer (nano ZS-90) based on dynamic light scattering (DLS) technique. The histogram shows narrow particle size distribution and the average particle diameter of 93.3 nm indicating that the aggregates are of nanoscale size. In order to obtain monodispersed aqueous suspension of nanoparticles with narrower particle size distribution the parameters like concentration of the solution, sonication time and temperature were optimized. The optimum values are i) concentration



Scheme 1. Schematic representation of synthesis of PHP.

of PHP in acetone = 5 mM, ii) sonication time = 30 min, and iii) temperature = 27 °C. The value of zeta (ζ) potential measured is -16.8 mV confer high level stability of nanoparticles. The aqueous suspension of nanoparticle with high zeta potential (negative or positive) is electrically stabilized while those with low zeta potentials tend to coagulate or flocculate [24]. The Scanning electron microscopy (SEM) image shown in Fig. 2 reveals that the PHPNPs are distinct spheres with similar size of 100 nm close to that estimated by DLS in support to monodispersed system.

3.2. Photophysical Properties of PHPNPs

Formation of nanoparticles in aqueous suspension is further confirmed by absorption and fluorescence spectroscopy. Fig. 3 presents absorption spectra of aqueous suspension of PHPNPs (A) and dilute solution of PHP in acetone (B). Absorption spectrum of dilute sample solution of PHP is banded with maximum at 442 nm while that of PHPNPs show broad peaks at 405 nm and 355 nm. The absorption transition $S_0 \rightarrow S_1$ is $\pi \rightarrow \pi^*$ because of conjugated phenyl ring and more number of delocalized π electrons. In contrast, the absorption spectrum of nanoparticle suspension is blue shifted from absorption spectrum of sample solution. The observed blue shift in absorption spectrum of PHPNPs indicates that the PHP molecules aggregate in planar cluster with contribution of individual molecules of H-type aggregates formed due to strong lateral π -stacking interaction. The fluorescence excitation and emission spectra of PHP in acetone and PHPNPs suspension are shown in Fig. 4. It is seen that the excitation spectrum of nanoparticles (Fig. 4 A.) is spectrally identical with absorption spectrum (Fig. 3 A.). The fluorescence spectrum of PHPNPs (C) is a broad, structureless band having enhanced emission at 506 nm and hypsochromically shifted by 2145.23 cm^{-1} from the isolated emission of single molecule (monomer) in acetone seen at 538 nm. The monomer emission peak is not seen in the spectrum of nanoparticle suspension. The emission spectrum of nanoparticle also shows high energy bands at 484 and 464 nm which are assigned to localized emission of the aromatic moiety. The strong enhanced emission at 506 nm is assigned to the most probable $\pi^* \rightarrow \pi$ transition owing to face to face π -stacking effect in nanoaggregates. Fig. 5 shows the decay profile of the dilute solution of

PHP in acetone (A) and the aqueous suspension of PHPNPs (B). It is known that aggregation and molecular interactions lead to a prolonged lifetime. The relatively longer lifetime of PHPNPs (4.26 ns) than that of PHP solution in acetone (1.58 ns) confirms that the PHPNPs molecules aggregate by self-assembly to form nanostructures and the characteristic enhanced emission of excited state nanoparticles appear at 506 nm. The long lifetimes of PHPNPs compared with that of a monomer solution are attributed to the formation of aggregated nanoparticles that restricts the molecular rotation and vibration of molecules and thus increases the emission lifetime of PHPNPs. The Stokes shift estimated as a difference between excitation and emission maxima of nanoparticles suspension ($\Delta\bar{\nu} = 5228.515 \text{ cm}^{-1}$) is higher than that of PHP solution in acetone ($\Delta\bar{\nu} = 4554.581 \text{ cm}^{-1}$). The larger Stokes Shift is evidence of strong intermolecular forces involving in aggregated nanostructures. The low emission intensity in solution of isolated molecule is due to dissipation of energy for molecular rotation. However, enhanced emission in nanoaggregates is because of the restricted molecular rotations and vibrations which prevent nonradiative decay and favors radiative pathway led to enhanced emission [25].

3.3. Effect of pH on Fluorescence Intensity of PHPNPs

The intensity of the Aggregation Induced Enhanced Emission (AIEE) of PHPNPs was seen to be influenced by pH of the aqueous suspension of nanoparticles. Carmody buffer was used to maintain pH of aqueous suspension of PHPNPs in the pH 2.0–12 range. Fig. 6 shows effect of pH on AIEE of PHPNPs. It is seen that fluorescence of nanoparticles is maximum when pH of solution is 7. While at low and high pH, intensity of fluorescence is less than maximum. The neutral range is observed to be suitable for the stability of PHPNPs in aqueous solution. At low and high pH the nanoparticles stability is affected by disruption of the cage of π -stacked H-aggregates of PHPNPs by which intensity of fluorescence is lowered. The optimum maximum fluorescence intensity is chosen at pH = 7 (neutral) which indicates a high power stability of nanoparticles. Therefore, in the present work pH 7.0 was maintained using phosphate as a buffer solution throughout the experiment.

3.4. Fluorimetric Recognition Test of PHPNPs for Metal Ions

The negative zeta potential -16.8 mV of PHPNPs in aqueous suspension indicates its ability to bind cations. The binding ability was examined by measuring changes produced in the fluorescence spectrum of PHPNPs after addition of aqueous solutions of metal ions prepared from their respective metal salts. Fig. 7 shows fluorescence spectra of aqueous suspension of PHPNPs recorded in the presence of metal ions viz. Sn^{2+} , Cu^{2+} , Fe^{3+} , Fe^{2+} , Ni^{2+} , NH_4^+ , Ca^{2+} , Pb^{2+} , Hg^{2+} and Zn^{2+} each of concentration 20 $\mu\text{g}/\text{mL}$. From the figure it is seen that presence of Sn^{2+} not only shifts the emission maxima but also increases the fluorescence intensity of PHPNPs while other cations respond oppositely and actually quench the fluorescence. The fluorescence intensity enhancement expressed as ratio $\Delta F/F$ of PHPNPs by Sn^{2+} and its comparison with other ions solution is presented as bar diagram in Fig. 8 (Red color bar). The enhancement in fluorescence, ΔF is the difference in the fluorescence intensity of PHPNPs in presence of metal ion (F) and in absence of metal ion solution (F_0). Fig. 8 (Violet bar) indicates that the presence of other ions with Sn^{2+} ion solution in PHPNPs does not

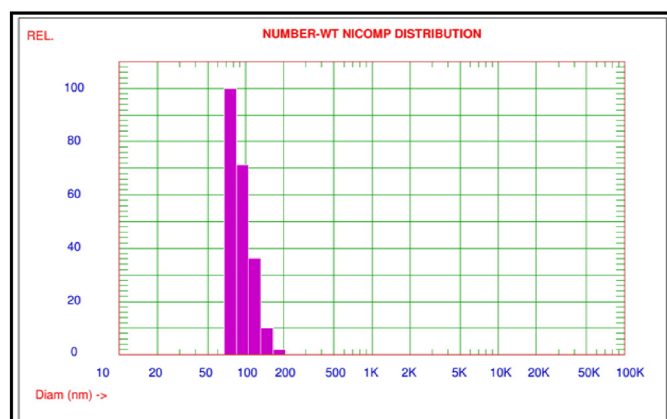


Fig. 1. Particle size distribution histogram of PHPNPs.

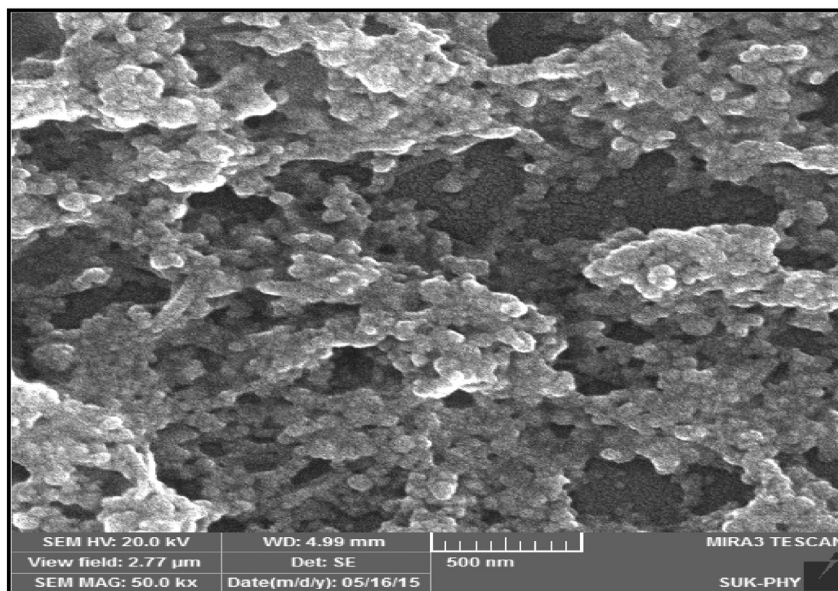


Fig. 2. SEM photomicrograph of PHPNPs.

interfere in the detection and fluorescence intensity response. The complexation of PHPNPs with Sn^{2+} increases the rigidity of the molecular assembly by restricted free rotations of the $-\text{OH}$ and $-\text{NH}$ group with respect to the phenyl rings results in a significant bathochromically shifted enhancement of the fluorescence intensity for PHPNPs. The selective fluorescent enhancement along with shift in emission maximum for PHPNPs by incremental addition of Sn^{2+} explained on the basis of strong electrostatic interaction between negatively charged surface of PHPNPs with the oppositely charged Sn^{2+} ion [26].

3.5. Fluorescence Titration of PHPNPs with Sn^{2+} and Calibration Curve

The fluorescence spectral changes of aqueous suspension of PHPNPs before and after addition of Sn^{2+} ion are depicted in Fig. 9. Small addition of Sn^{2+} solution significantly quenches the AIEE of PHPNPs at 532 nm and new broad structureless emission band appearing in the region 540–560 nm with maximum at 552 nm. Further addition of Sn^{2+} solution increases the intensity of this new emission band. The analytical relationship established by plotting increase in intensity of fluorescence (ΔF) versus concentration of Sn^{2+} solution is shown in Fig. 10. The experimental data of enhancement of fluorescence by Sn^{2+} fits

well into the linear relationship in the range of concentration 0–40 $\mu\text{g}/\text{mL}$ and the correlation coefficient of R^2 is 0.992. The limit of detection [8–10] is calculated by Eq. (1)

$$LOD = \frac{3.3\sigma}{k} \quad (1)$$

where, σ is the standard deviation of the y-intercepts of the regression lines and k is the slope of calibration graph. The estimated value of LOD is 0.0027 $\mu\text{g}/\text{mL}$ (2.27 μM) and in comparison with other method of detection of Sn^{2+} is appreciably lower [21,27].

3.6. Mechanism of Binding of PHPNPs with Sn^{2+}

Sn^{2+} ions are believed to be adsorbed and bind with the negatively charged surface of PHPNPs. The interaction occurs due to electrostatic forces of attraction between nanoprobe and Sn^{2+} . The mechanism of binding was discussed on the basis of the Langmuir adsorption concept [10,11,28]. The rate of binding of Sn^{2+} ion to the nanoparticle surface (R_b) is proportional to their concentration (C) in the analyte solution

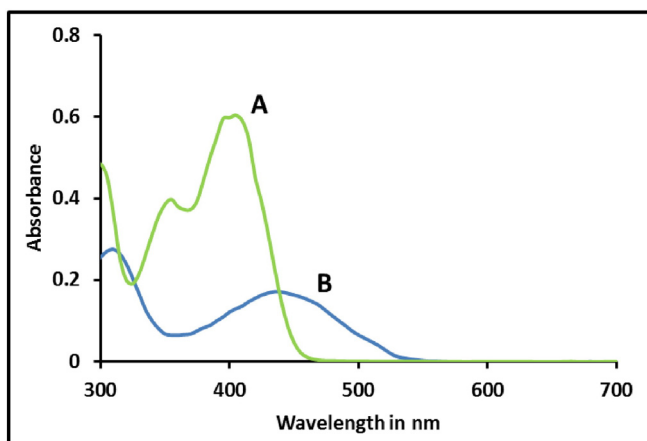


Fig. 3. Absorption spectra of PHPNPs (A) and solution of PHP in acetone (B).

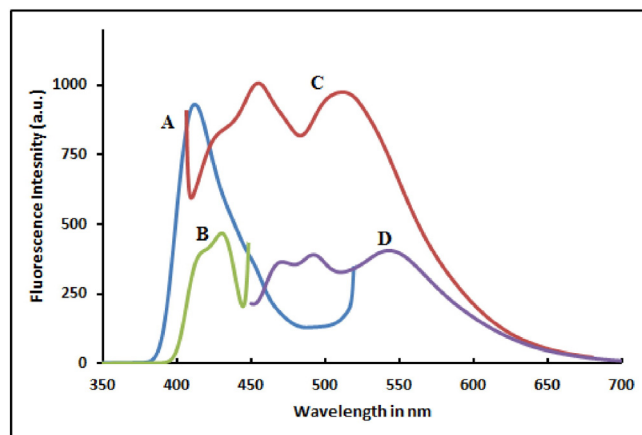


Fig. 4. Excitation spectra of PHPNPs suspension (A) and of dilute solution of PHP in acetone (B) and fluorescence spectra of PHPNPs suspension (C) and dilute solution of PHP in acetone (D). [For PHPNPs: ($\lambda_{em} = 506$ nm, $\lambda_{ex} = 405$ nm) and for PHP in acetone: ($\lambda_{em} = 538$ nm, $\lambda_{ex} = 425$ nm)].

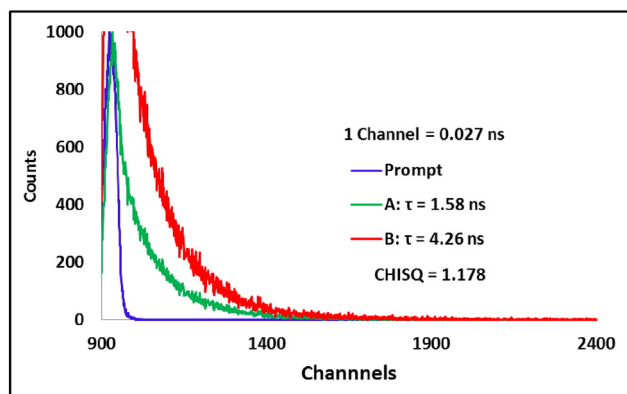


Fig. 5. Fluorescence decay profile of prompt (standard) solution, dilute solution of PHP in acetone (A) and PHPNPs suspension (B).

and the fraction of available binding sites is $(1-\theta)$; where, θ is defined as the fraction of occupied states.

$$R_b = K_b \times C(1-\theta) \quad (2)$$

Similarly, the rate of desorption of bound Sn^{2+} from the nanoparticle surface depends only on the fraction of the occupied binding sites and is expressed as,

$$R_d = K_d \times \theta \quad (3)$$

At equilibrium, the rate of binding is equal to rate of desorption K_d

$$K_d \times \theta = K_b \times C(1-\theta) \quad (4)$$

where, K_b and K_d are the binding and desorption constant of Sn^{2+} ions. The above equations solved as function of the ratio as,

$$B = \frac{K_b}{K_d} \quad (5)$$

$$\theta = \frac{BC}{1+BC} \quad (6)$$

The fraction of occupied binding sites (θ) is related to the ratio of the fluorescence signal obtained (F) at given Sn^{2+} concentration and the fluorescence intensity (F_0) without Sn^{2+} solution and is expressed as,

$$\theta = \frac{F}{F_0} = \frac{BC}{1+BC} \quad (7)$$

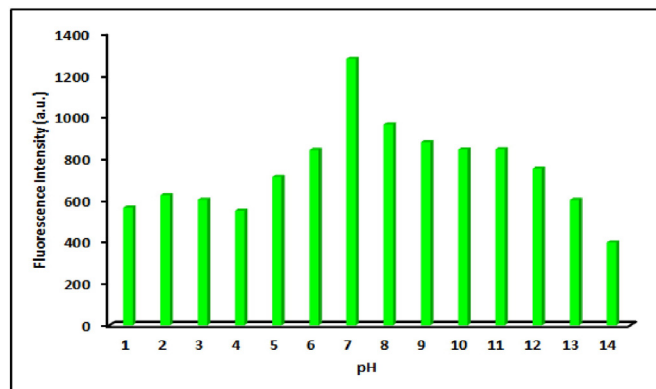


Fig. 6. Effect of pH on fluorescence intensity of PHPNPs suspension.

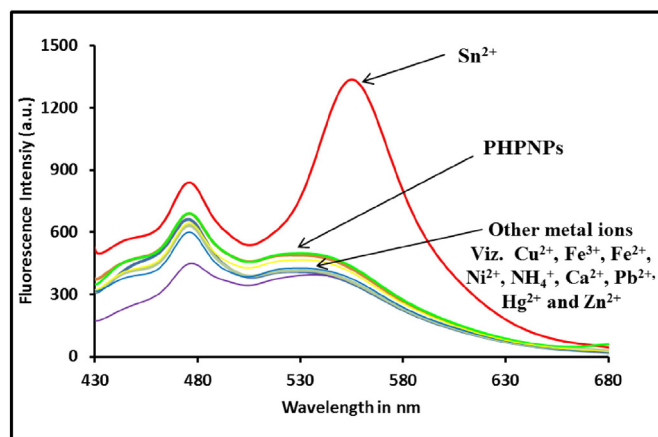


Fig. 7. Selectivity of PHPNPs towards Sn^{2+} shows fluorescence enhancement than other cations viz. Cu^{2+} , Fe^{3+} , Fe^{2+} , Ni^{2+} , NH_4^+ , Ca^{2+} , Pb^{2+} , Hg^{2+} and Zn^{2+} of concentration $20 \mu\text{g/mL}$ each ($\lambda_{\text{ex}} = 405 \text{ nm}$).

Eq. (8) can be linearized to take the form,

$$\frac{C}{F} = \frac{1}{BF_0} + \frac{1}{F} C \quad (8)$$

Eq. (8) is the linear form of the Langmuir adsorption equation. The linearized plot of C/F vs. concentration of Sn^{2+} ions added (C) is shown in Fig. S5†. The adsorption equilibrium constant (B) is the Langmuir binding constant (K) given by the slope and the intercept of the linear plot. Hence, according to the Langmuir adsorption description, the binding of Sn^{2+} on the surface of nanoparticles can be examined by the plot of C/F as a function of concentration (C) of the Sn^{2+} ion solution added and as per the expectation this plot is linear as given in Fig. S5†. The coefficient of linear fit is 0.992 and the Langmuir binding constant K is $3.112 \times 10^5 \text{ M}^{-1}$. The adsorption results led to considering that the enhancement of fluorescence of PHPNPs is because of the binding of adsorbed Sn^{2+} on the nanoparticle surface. In addition to this, the results of the DLS-Zeta sizer support the adsorption of Sn^{2+} ion on the nanoparticle surface. The bar diagram in Fig. S6† shows variation of the zeta potential and the size of PHPNPs in presence of the different concentration of Sn^{2+} solution. It can be seen that the negative zeta potential of the nanoparticle/water interface decreases successively from -16.8 mV to -14.2 mV and -12.2 mV and the particle size increases from 93.3 nm to 245.6 nm and 521.7 nm upon addition of $20 \mu\text{g/mL}$ and $40 \mu\text{g/mL}$ solutions of Sn^{2+} ion respectively. These observations suggested the adsorption of Sn^{2+} ions over the negatively charged

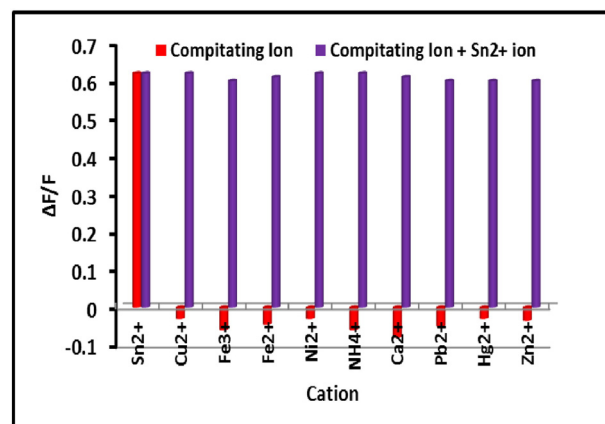


Fig. 8. Bar diagram showing fluorescence intensity response $[(\Delta F)/F]$ of PHPNPs in the presence and absence of the Sn^{2+} ion and several coexisting anions like Cu^{2+} , Fe^{3+} , Fe^{2+} , Ni^{2+} , NH_4^+ , Ca^{2+} , Pb^{2+} , Hg^{2+} and Zn^{2+} of concentration $20 \mu\text{g/mL}$ each.

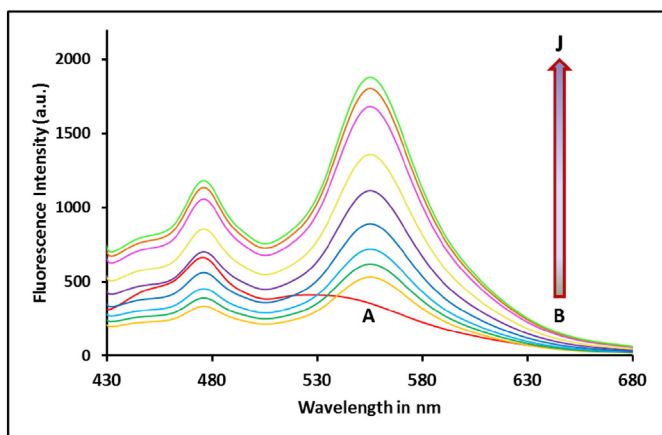


Fig. 9. Fluorescence spectra of PHPNPs suspension in the presence of different concentrations of Sn^{2+} ions (A to J) (A: 0 $\mu\text{g}/\text{mL}$, B: 5 $\mu\text{g}/\text{mL}$, C: 10 $\mu\text{g}/\text{mL}$, D: 15 $\mu\text{g}/\text{mL}$, E: 18 $\mu\text{g}/\text{mL}$, F: 20 $\mu\text{g}/\text{mL}$, G: 25 $\mu\text{g}/\text{mL}$, H: 30 $\mu\text{g}/\text{mL}$, I: 34 $\mu\text{g}/\text{mL}$, J: 40 $\mu\text{g}/\text{mL}$) ($\lambda_{\text{em}} = 552 \text{ nm}$, $\lambda_{\text{ex}} = 405 \text{ nm}$).

surface of nanoparticles. The UV–visible spectra of PHPNPs shown in Fig. S7† indicate that the presence of various concentrations of Sn^{2+} does not produce a spectral shift rather only induce increase in absorption of PHPNPs. This observation ignores the possibility of ground state complexation and led to consider excited state complexation between negatively charged nanoparticles and Sn^{2+} ion. The excited state complexation involves binding of Sn^{2+} ions to PHPNPs by a bond through $-\text{OH}$ and $-\text{NH}$ groups in PHPNPs by electrostatic forces which leads into enhanced emission of nanoparticles and thus favors the restricted intramolecular rotations. The observed fluorescence enhancement of PHPNPs is further supported by fluorescence lifetime of PHPNPs measured in the presence of 10, 20 and 40 $\mu\text{g}/\text{mL}$ of Sn^{2+} ion solution was obtained and decay profile shown in Fig. 11. The lifetime 4.26 ns of PHPNPs without Sn^{2+} found to increase to 6.71 ns in presence of increasing concentration of Sn^{2+} solution of 10 $\mu\text{g}/\text{mL}$, 20 $\mu\text{g}/\text{mL}$ and 40 $\mu\text{g}/\text{mL}$. It is known that the aggregation and molecular interactions lead to prolonged fluorescence lifetime [29,30]. The increase in lifetime of PHPNPs with addition of Sn^{2+} suggests increased stabilization of excited complex. All these observations led us to consider that excited state complexation formed in between PHNPs and Sn^{2+} ion in aqueous solution. The schematic representation of plausible mechanism of fluorescence enhancement based on Sn^{2+} ion adsorption on the surface of PHPNPs is graphically represented in Scheme 2.

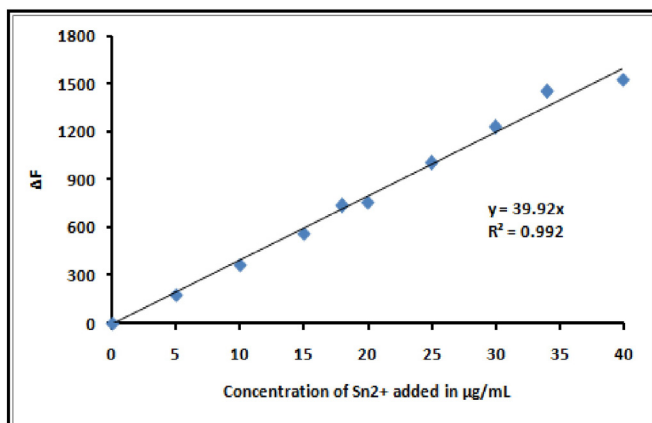


Fig. 10. Plot of ΔF as function of concentration of Sn^{2+} ion.

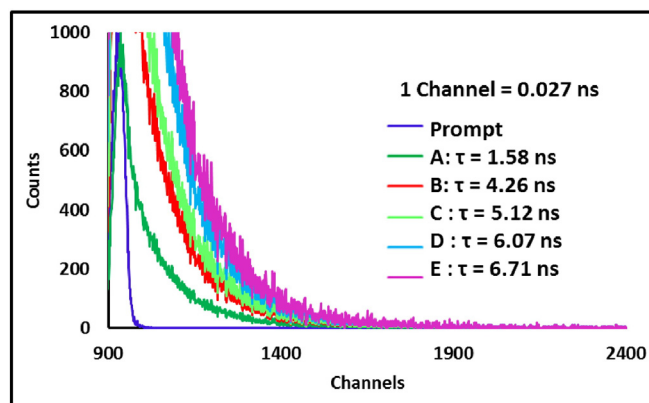


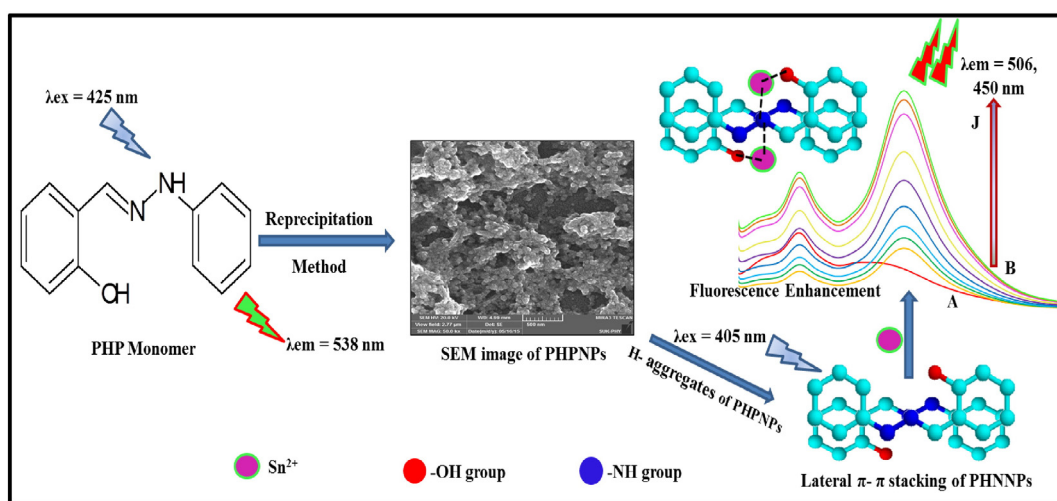
Fig. 11. Fluorescence decay profile of prompt (standard) dilute solution of PHP in acetone (A), PHPNPs suspension (B) and increasing concentration of Sn^{2+} ion solution to PHPNPs suspension (C: 10 $\mu\text{g}/\text{mL}$, D: 20 $\mu\text{g}/\text{mL}$, E: 40 $\mu\text{g}/\text{mL}$).

3.7. Application of Proposed Method for Natural Samples Analysis

The fluorescence enhancement of PHPNPs by Sn^{2+} was further used to develop an analytical method for quantitative determination of Sn^{2+} from environmental real water samples. The method includes determination of Sn^{2+} ions in water samples collected from adjacent local area of Shivaji University campus, Kolhapur (SUK), Maharashtra, India. For the better results and analysis of Sn^{2+} ion in the environmental samples, the collected samples had undergone pretreatment for sample purification to avoid the interference of other impurities and matrix in the environmental samples. The samples collected were first filtered through Whatmann filter paper no. 41 to remove suspended matter and impurities, followed by boiling for 10 min to remove chlorine and dissolved gases. The collected environmental samples were spiked with standard Sn^{2+} ion solution of three concentration levels and diluted within the working range. The sample was analyzed by the proposed fluorimetric method using calibration curve shown in Fig. 10. The recovery of Sn^{2+} ion added in environmental samples was calculated and the results are summarized in Table 1. It can be seen that the value of Sn^{2+} found in the two concentration level is identical with expected values. The recovery and relative standard deviation are very satisfactory and imply the suitability of present method for quantitative determination of Sn^{2+} from environmental real water samples.

4. Conclusion

The fluorescent 2-[(E)-(2-phenylhydrazinylidene)methyl]phenol (PHP) compound was synthesized and characterized using IR, NMR and MS. Further, it was used to prepare fluorescent nanoparticles using reprecipitation (PHPNPs) method which exhibits narrower particle size distribution showed by DLS histogram. The SEM examination indicated spherical shaped morphology. The UV–visible absorption and fluorescence spectroscopy results indicated the H-bonded aggregates involving π -stacking and strong AIEE is arising due to hindered molecular rotations thus favoring radiative decay of nanoaggregates. The negative zeta potential and affinity of $-\text{OH}$ and $-\text{NH}$ groups introduce strong and selective binding of PHPNPs with oppositely charged Sn^{2+} resulting into enhancement in fluorescence intensity of nanoparticles. The observed red shifted AIEE of PHPNPs in presence of Sn^{2+} was discussed on the basis of electrostatic interactions between oppositely charged nanoprobe and analyte (Sn^{2+}) introduces excited state complexation between them. The fluorescence enhancement and binding mechanism was supported by UV–visible titration, fluorescence titration, Langmuir adsorption plot, DLS-Zeta sizer and fluorescence lifetime studies. The results of fluorescence enhancement in PHPNPs with addition of Sn^{2+} fits into the straight line equation with RSD = 0.992%. The present method



Scheme 2. Proposed graphic for formation of PHPNPs and its complexation with Sn^{2+} ion.

Table 1

Determination of Sn^{2+} in different environmental water samples.

Water samples studied	Amount of standard Sn^{2+} ion added ($\mu\text{g}/\text{mL}$)	Total Sn^{2+} ion found ($\mu\text{g}/\text{mL}$) (n = 3)	Recovery of Sn^{2+} ions added (%)	RSD(%)	Relative error (%)
Rajaram Lake, Near	15	14.94	99.60	0.012	-0.004
SUK.	25	24.98	99.92	0.014	-0.0008
Panchaganga River,	35	34.99	99.97	0.017	-0.0003
Kolhapur	15	14.97	99.80	0.011	-0.002
	25	24.99	99.96	0.012	-0.0004
	35	34.95	99.85	0.014	-0.0015

*n = Average of three determinations.

has lower Limit of Detection (LOD) = $0.0027 \mu\text{g}/\text{mL}$ ($2.27 \mu\text{M}$) for Sn^{2+} as compared to other traditional methods reported so far for Sn^{2+} . The present method was used to develop fluorimetric method for determination of Sn^{2+} in environmental samples collected from local area. The method affords fairly practical and economical approach.

Appendix A. Supplementary data

Supplementary data to this article can be found online at <http://dx.doi.org/10.1016/j.saa.2016.07.020>.

References

- [1] Y. Xiang, L. Mei, N. Li, A. Tong, *Anal. Chim. Acta* 581 (2007) 132–136.
- [2] C. Li, F. Xu, Y. Li, K. Zhou, Y. Zhou, *Anal. Chim. Acta* 717 (2012) 122–126.
- [3] X. Chen, L. He, Y. Wang, B. Liu, Y. Tang, *Anal. Chim. Acta* 847 (2014) 55–60.
- [4] Z. Chen, D. Wu, *Sensors Actuators B Chem.* 192 (2014) 83–91.
- [5] V.K. Bhardwaj, H. Sharma, N. Kaur, N. Singh, *New J. Chem.* 37 (2013) 4192–4198.
- [6] A. Farooq, R. Al-Jowder, R. Narayanaswamy, M. Azzawi, P.J.R. Roche, D.E. Whitehead, *Sensors Actuators B Chem.* 183 (2013) 230–238.
- [7] N. Kaur, S. Kaur, R. Mehan, C. Aguilar, P. Thangarasu, N. Singh, *Sensors Actuators B Chem.* 206 (2015) 90–97.
- [8] P.G. Mahajan, D.P. Bhopate, G.B. Kolekar, S.R. Patil, *J. Fluoresc.* (2016), <http://dx.doi.org/10.1007/s10895-016-1839-7>.
- [9] P.G. Mahajan, D.P. Bhopate, G.B. Kolekar, S.R. Patil, *Sensors Actuators B Chem.* 220 (2015) 864–872.
- [10] P.G. Mahajan, D.P. Bhopate, A.A. Kamble, D.K. Dalavi, G.B. Kolekar, S.R. Patil, *Anal. Methods* 7 (2015) 7889–7898.
- [11] P.G. Mahajan, N.K. Desai, D.K. Dalavi, D.P. Bhopate, G.B. Kolekar, S.R. Patil, *J. Fluoresc.* 25 (2015) 31–38.
- [12] (a) C.A. Huerta-Aguilar, T. Pandiyan, P. Raj, N. Singh, R. Zanella, *Sensors Actuators B Chem.* 223 (2016) 59–67;
(b) S.J. Chopra, J. Singh, H. Kaur, N. Singh, N. Kaur, *Sensors Actuators B Chem.* 220 (2015) 295–301.
- [13] V.K. Gupta, N. Mergu, L. Kumawat, A. Singh, *Talanta* 144 (2015) 80–89.
- [14] V. Bhalla, A. Gupta, M. Kumar, *Org. Lett.* 14 (2012) 3112.
- [15] L. Jinshui, W. Lun, G. Feng, L. Yongxing, W. Yun, *Anal. Bioanal. Chem.* 377 (2003) 346–349.
- [16] M. Yildirim, I. Kaya, *J. Fluoresc.* 20 (2010) 771–777.
- [17] Z. Yurtman, C. Gündüz, C. Özpinar, O. Aydın Urucu, *Spectrochim. Acta A Mol. Biomol. Spectrosc.* 136 (2015) 1679–1683.
- [18] X. Cheng, M. Wang, Z. Yang, Y. Li, T. Li, C. Liu, Q. Zhou, *J. Coord. Chem.* 66 (2013) 1847–1853.
- [19] L.J. Fan, W.E. Jones, *J. Am. Chem. Soc.* 128 (2006) 6784.
- [20] L. Lin, L. W. Fang, Y. Yu, R. Huang, L. Zheng, *Spectrochim. Acta A* 67 (2007) 1403–1406.
- [21] X. Bao, X. Cao, X. Nie, Y. Jin, B. Zhou, *Molecules* 19 (2014) 7817–7831.
- [22] D.K. Das, P. Goswami, P. Sarma, *J. Fluoresc.* 23 (2013) 503–508.
- [23] S.A. Ghosh, A. Alam, A. Gangulya, N. Guchhait, *Spectrochim. Acta A* 149 (2015) 869–874.
- [24] J. Lyklema, *Fundamentals of Interface and Colloid Science*, Elsevier, Wageningen, 1995.
- [25] F. Wang, M. Han, K. YiMya, Y. Wang, Y. Lai, *J. Am. Chem. Soc.* 127 (2005) 10350–10355.
- [26] A. Ciferri, A. Perico, *Ionic Interactions in Natural and Synthetic Macromolecules*, first ed. Vol. 2, John Wiley & Sons Inc. Publication, 2012.
- [27] L. Lin, W. Fang, Y. Yu, R. Huang, L. Zheng, *Spectrochim. Acta A* 67 (2007) 1403–1406.
- [28] J. Hou, L. Wang, D. Li, X. Wu, *Tetrahedron Lett.* 52 (2011) 2710–2714.
- [29] M.Y. Berezinand, S. Achilefu, *Chem. Rev.* 110 (2010) 2641–2684.
- [30] M. Cai, Z. Gao, X. Zhou, X. Wang, S. Chen, Y. Zhao, Y. Qian, N. Shi, B. Mi, L. Xie, W. Huang, *Phys. Chem. Chem. Phys.* 14 (2012) 5289–5296.